Further insights into release mechanisms from nano-emulsions, assessed by a simple fluorescence-based method

Xinyue Wang, Mayeul Collot, Ziad Omran, Thierry Vandamme, Andrey Klymchenko, Nicolas Anton

Further insights into release mechanisms from nano-emulsions, assessed by a simple fluorescence-based method

Xinyue Wang,[a] Mayeul Collot,[b] Ziad Omran,[c] Thierry F. Vandamme,[a] Andrey Klymchenko,[b] Nicolas Anton[a,*]

[a] *Université de Strasbourg, CNRS, CAMB UMR 7199, F-67000 Strasbourg, France*

[b] *Université de Strasbourg, CNRS, LBP UMR 7021, F-67000 Strasbourg, France*

[c] *Department of Pharmaceutical Chemistry, College of Pharmacy, Umm AlQura University, 21955 Makkah, Kingdom of Saudi Arabia*

Abstract

Nano-emulsion consists of a dispersion of oil droplets sizing below 200 nm, in aqueous continuous phase, and generally stabilized by low-molecular weight surfactants. These stable nano-carriers are able to encapsulate and transport lipophilic molecules poorly soluble in water. However, the question on the leakage and release mechanisms of an active pharmaceutical ingredient, from oil nano-droplets to an acceptor medium has not been clearly addressed. Herein, we developed a simple fluorescence approach based on self-quenching of lipophilic fluorophore based on Nile Red (NR668) to monitor cargo transfer from lipid nano-droplets to the acceptor medium. In this method, the fluorophore release can be monitored by the increase in its fluorescence quantum yield and the blue shift in its emission spectrum. The studies of the release process allow emphasizing an important role the bulk aqueous medium in controlling the droplet to droplet fluorophore transfer and the attained equilibrium. The developed methodology could be applied to monitor release of other lipophilic dyes and it could help to better understand the cargo release from nanocarriers.

Introduction

Nano-emulsion (NE) is nano-scaled biphasic dispersion of two immiscible liquids stabilized by amphiphilic molecules. Owing to the high surface area, good physico-chemical stability and non-toxicity, NEs are becoming a promising carrier in many application fields, such as the drug delivery, diagnostic, cosmetic, pesticide and food industries [1-5]. Compared to other types of nano-carriers, NEs have a real advantage to be a liquid reservoir for lipophilic active pharmaceutical ingredients (APIs), and thus, *a priori*, lipophilic fluorescent probes as models. This original feature has recently allowed the encapsulation of an outstanding number of fluorophores in a single droplet, making ultrabright nano-droplets enabling new possibilities such as single droplet tracking in cells or in small laboratory animals [6-8]. Although a large number of literature reports has shown that NE droplets themselves are intrinsically very stable, shown experimentally [9, 10], and explained by the fact that droplets cannot enter in contact each other for steric reasons [11-13], the important question of the leakage of encapsulated APIs is still not clearly addressed.

Literature [6, 14, 15] showed that lipophilic APIs encapsulated in nano-emulsion can present very different release properties and stability, related to their chemical structure, lipophilicity, and affinities for the acceptor medium. In storage conditions, this leakage is generally negligible, as such lipophilic APIs are not soluble in aqueous medium. However, when the nano-carriers are brought into contact with an acceptor medium, such as serum, cells, biological tissues, or blank oil nano-droplets (oil droplets without API), a partitioning of the encapsulated molecules can occur, driving their leakage from the initial droplets to the acceptor reservoirs. Based on comparable phenomenon, at different concentration scales, this phenomenon can gather the so-called *compositional ripening* in which droplets of different compositions (like loaded and blank droplets) tend to equilibrate their concentration. In contrast to *Ostwald ripening*, *compositional ripening* has not been extensively investigated, likely due to the fact that its monitoring is not trivial on an experimental point of view [14, 16]. However, understanding and controlling the stability of APIs encapsulation, up to the nano-carrier reaches the targeted site, is crucial, and it is not rare to see literature reports in which it is simply assumed, while a partial or complete leakage has already occurred.

In this study, we have considered that studying the stability of APIs encapsulated in nano-emulsion droplets can be extrapolated as a partial compositional ripening in which only APIs are able to release. The main mechanism at the origin of Ostwald and compositional ripening is the transfer of the dispersed phase through the continuous one, even if the oil is considered as *insoluble in* water, a very low solubility still allows such an inter-droplet molecular transfer. Indeed, in Ostwald ripening studies, the ripening rate was closely related to the solubility of the oil in water [17], and described by three possible mechanisms: a) a

mechanism simply governed and limited by the molecular diffusion without any energy barrier [18, 19]; b) the diffusion-limited mechanisms can be helped by micelles formed in the aqueous bulk acting as the carriers of oil molecules [17, 20]; c) the mass transfer between droplets is controlled by an energy barrier related to an interfacial resistance or to the bulk phase properties [21-24].

Recent works investigated the mass transfer between micrometric droplets focusing on complex emulsions like Pickering emulsions [25] and multiple emulsions [26], helped by developments of optical imaging with high-resolution cameras [27]. However, these experiments were conducted on macro or micro-scale emulsions, but not adaptable on nano-emulsions reaching the limit of such experimental approach. Fluorescence techniques like Förster Resonance energy transfer (FRET) are particularly suitable for studying molecular transfer of lipophilic cargo, where the dye leakage is identified as the loss of FRET between the donor and acceptor cargo molecules, however requiring a double fluorescence labelling of nanoemulsions [28]. Fluorescence correlation spectroscopy, a recently proposed strategy which uses a single fluorescent lipophilic cargo can detect the cargo transfer through change in brightness and concentration of emissive species, as well as by monitoring standard deviation of fluorescence fluctuations [14], however, requires a dedicated fluorescence microscopy setup.

In this study, we propose a new approach to quantify and follow the stability, behavior and release of a model API (lipophilic fluoroprobe) based on the model of compositional ripening. The water-insoluble fluorescent NR668 (lipophilic Nile red derivative) encapsulated in nano-emulsion droplets, at a concentration high enough to induce a self-quenching of the probes due to molecular stacking, thus reducing its fluorescence quantum yield (QY). This phenomenon is reversible and decreases upon the dilution of the probes. Therefore, as their leakage towards an acceptor medium occurs, the QY increases and stabilizes when the concentration is equilibrated among all the donors and acceptors. The stability and robustness of this system will allow for clear identification of the conditions which can initiate the leakage, along with their respective impact. Herein, we propose a novel methodology to quantify the molecular leakage and kinetics from nano-carriers not subjected to Ostwald ripening, as well as give novel insights on the formulation parameters impacting on these phenomena.

Materials and Methods

Materials

The oil phase, vitamin E acetate (VEA), was provided by Tokyo Chemical Industry (Tokyo, Japan). The surfactant, Kolliphor ELP®, was purchased from BASF (Ludwigshafen, Germany). NR668 is a homemade modified Nile Red fluorophore on which was grafted lipophilic chains. Milli-Q water was obtained from a Millipore filtration system and used in all experiments.

Methods

Preparation of nanoemulsions and micelles

NR668-loaded NEs were prepared by spontaneous emulsification method. Firstly, NR668 was dissolved in VEA with different loadings of 1%, 2% and 3% in mass fraction. The dye-in-oil mixture was heated to 80 °C and mixed at 2,000 rpm with a thermomixer (Eppendorf), and vortexed (Bioblock Scientific) until the full solubilization and homogenization. After that, 200 mg of the mixture was centrifuged (Eppendorf) at 13,000 rpm for 1 min in case there could be some residues on the wall. Next, 200 mg Kolliphor ELP® was added, following the same mixing and vortex. With the addition of 600 µl Milli-Q water (at 80 °C) after mixing at room temperature for 10 minutes, the highly concentrated NEs were prepared. The choice of NR668 —a lipophilic version of Nile Red (NR)— came from its greater stability against leakage compared to NR, when the water continuous phase is replaced for an acceptor medium like serum, cells or biological tissues like zebra-fish [6-8]. In addition, this choice was also driven by its fluorescent properties: when NR668 is dispersed in water there is almost no fluorescent signal, while it increases by 681-fold when solubilized in vitamin E acetate (structure and spectra of NR668 in water and VEA are reported in Fig. S1 in *Supplementary information* section).

Blank NEs were prepared with the same procedure above except that no dye was encapsulated. Blank micelles were prepared by mixing 200 mg Kolliphor ELP® with 800 mg Milli-Q water at the same condition.

Owing to the high percentage of surfactant used during the preparation of NEs, some micelles could be present in the bulk solution. In some cases, in order to eliminate the interference of micelles on droplet-droplet mass transfer and to compare the difference with or without micelles, dialysis was used to separate the large droplet from micelles. Regenerated cellulose dialysis membrane with a molecular weight cut off 12-14 kDa was provided by Spectrumlabs® (Rancho Dominguez, USA). Dialysis was conducted for 48 h at room temperature with Milli-Q water as the outer phase, and it was changed every 24 h.

Mass transfer kinetics

Before the kinetic study, all the solutions were diluted with 100 times in ultrapure water to ensure a moderate transfer rate. The dilution and mixing process were shown in detail in Fig. 1. After that, the mixture was incubated in a thermomixer at the lowest speed (300 rpm) for 5 h. At each time point, 20 µl samples were taken, diluted again (10 times) and kept at 4 °C immediately to stop the transfer process. All the experiments were triplicated.

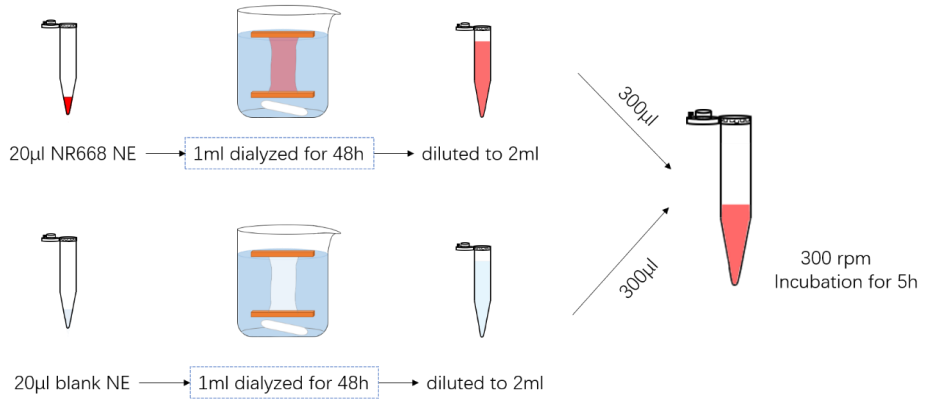

Figure 1: Schematic representation of the preparation of loaded (top) and blank (bottom) droplets before mixing them together to study the dye molecular transfer between each other.

Absorption and fluorescence spectra

Absorption and fluorescence spectra were measured with a Cary 4000 HP ultraviolet-visible spectrophotometer (Agilent Technologies) and a Fluoromax-4 spectrofluorometer (Horiba Scientific), respectively. The absorption spectra were scanned from 400 nm to 700 nm, while the emission spectra were recorded from 490 nm to 700 nm with an excitation wavelength of 480 nm. All the solutions used for the spectral measurement were diluted to a dye concentration around 1 µM, where the absorption is below 0.1 for QY measurement. For the quantum yield calculation, Rhodamine 6G in water [29] was used as the reference.

When concentration of NR668 in nano-droplets is high, a phenomenon of *aggregation-caused quenching* (ACQ) occurs and results in a loss of the fluorescence efficiency. This consequences in decreasing the QY [30], and in a slight shift of the fluorescent spectra. Quantum yield is an important parameter to characterize fluorescent efficiency, which is defined as the ratio of the number of photons emitted to the number of photons absorbed:

$$\mathrm{QY} = \frac{OD_R \times I \times n^2}{OD \times I_R \times n_R^2} \times \mathrm{QY}_R \qquad (1)$$

where QY represents quantum yield, OD is the optical density at excitation wavelength of 480 nm, I is the integrated fluorescence intensity, n is the refractive index of the solvent (*i.e.* water, n = 1.33). . Quantum yield is a measure of the efficiency of photon emission and cannot reach more than 100%. It was measured using a reference, rhodamine 6G, defined with a QY of 95% in water. Accordingly, the measured QY values were expressed in the scale range of 0 to 100%.

In our case, when dye molecules were transferred from a highly concentrated oily core to a blank emulsion droplet, the dilution will induce a reduction of the self-quenching and therefore an increase in the QY. By using this method based on the determination of the QY, the molecular mass transfer can be followed-up simply by fluorescence spectroscopy, and whatever the -micro or nano- scale of

the dispersion. In addition, the fluorescence spectra can be shifted with the polarity of the acceptor medium (*i.e.* blank nano-droplets or micelles suspension), reflecting the transition before reaching the equilibrium.

Characterizing nanodroplet size distribution

After spectra measurement, size of all the samples were tested by Dynamic Light Scattering with the instrument Zetasizer® Nano ZS (Malvern). Both size distribution and polydispersity index (PDI) were recorded at a temperature of 25° C. All the samples were performed in triplicate.

Results

Impact of formulation parameters on mass transfer

As introduced in the previous sections, a new methodology was developed to study the encapsulation stability, the molecular leakage and transfer from the donor to the acceptor medium. This methodology involved following up the fluorescence QY and the shift of the emission maximum during the process.

Focus on the type of acceptor medium

In this section, the idea was to study the leakage of a model dye (NR668), comparing different lipid acceptor media for varied donor/acceptor ratios and temperatures. The donor nano-droplets were also varied as native and dialyzed NEs. The objective of this first screening is to understand general rules that can significantly impact the leakage mechanisms. Different types of acceptor media were studied: *(i)* native formulation of blank NEs, with an excess of surfactant in the bulk forming micelles (which is associated with the emulsification process); *(ii)* blank dialyzed NEs without micelles, where the excess of surfactant was removed by dialysis; *(iii)* acceptor media in form of only micelles; *(iv)* blank dialyzed NEs with micelles, where surfactant was reintroduced after dialysis at the same concentration as used in the formulation of blank nano-emulsion; and *(v)* control, where the acceptor medium is only distilled water. For all experiments, two donor/acceptor ratios were selected (1/1 and 1/2), and two temperatures were compared (60° C and 80° C). Similar experiments at room temperature do not show any release (these results will be shown and discussed below on the *focus on the effect of temperature* subsection). The presence of micelles in the continuous phase comes from the spontaneous emulsification process, involving a surfactant concentration largely higher than the CMC (0.02 wt.% in water at 37° C, given by the manufacturer BASF).

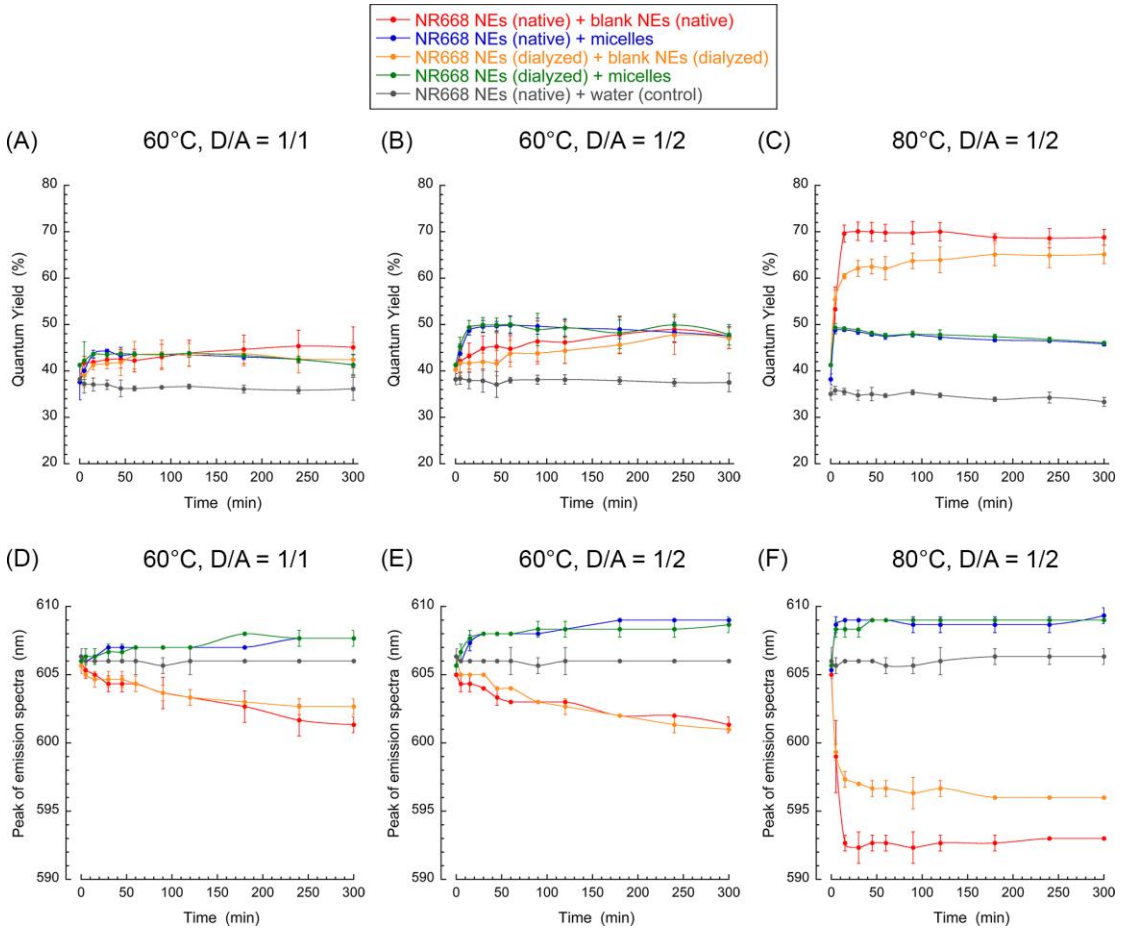

Figure 2: Study of the quantum yield (A,B,C) and values of the peak of the fluorescence spectra (D,E,F) for different experimental conditions of temperature (60° C and 80° C) and donor-to-acceptor ratio (1/1 and 1/2), indicated in the figure, with the dye concentration in oil equal to 3 wt.%.This experiment was conducted for different systems varying in the nature and composition of the acceptor (see details in the text). Data are mean values, and error bars indicate ± standard deviation, n = 3.

The results, reported in Fig. 2, show the evolution of QY and spectral shift (peak values are reported) over time. The corresponding spectra are reported in the *Supplementary information* section as Fig. S2, S3 and S4. The first remark concerns the control experiment with Milli-Q water (gray curves), where both QY and peak value remain constant all over the experiments whatever the temperatures are. In that case, we can consider that there is no acceptor medium, and these results confirm the stability of the NEs and also the conservation of the dye properties over the experiment. On the other hand, once acceptors are introduced in the medium, these stability profiles are significantly modified compared to the control with Milli-Q water.

The significant difference was obtained when comparing the acceptor medium composed of blank nano-emulsion droplets and micelles (without droplets), but indeed not in all the conditions studied. At first, in Fig. 2 (A) (60° C and

D/A = 1/1), all acceptors induce a slight increase of the QY values at around 6% compared to the water control. This is confirmed by a slight shift of the peak values in Fig. 2 (D), where the curves are shifted towards the blue (decreasing the wavelength) when the acceptor medium is a droplet suspension, and towards red (increasing the wavelength) when the acceptor medium is the micelles suspension. In contrast to variations of QY (related to dye self-quenching), the shift of the dye spectrum is due to its solvatochromism. This is thus revealing modifications of the polarity of the solubilizing medium [31]. A lose or increase of the acceptor polarity indicates that acceptor medium is the oil core of nano-droplets, or the micelles, respectively. Thus, the proper fact that polarity of acceptor medium has changed is also a confirmation of the leakage of the dyes.

The observed effects are enhanced when the concentration of acceptors is doubled, where for the same temperature, the QY values rapidly increases to stabilize around 10% compared to the water control, a value higher than for the previous conditions (Fig. 2 (B), 60° C and D/A = 1/2). Interestingly, when the acceptor medium is only made of micelles, the kinetics are faster compared to droplets, but the intensity values finally stabilize at the same above-mentioned value. As regards the spectra shifts (Fig. 2 (E)), similar results to the previous conditions (Fig. 2 (A), 60° C and D/A = 1/1) were obtained, with blue and red shifts for droplets and micelles, respectively. Finally, raising the temperature up to 80° C results in a clear additional effect on the QY (Fig. 2 (C)) and spectra shift (Fig. 2 (F)) for the acceptor medium made of droplets, reaching around 35% compared to the water control, while this temperature has no impact when the acceptor is only composed of micelles.

Interestingly, the NEs dialysis appears to have a significant inhibiting effect on the curves(difference between red and orange curves, native and dialyzed, respectively). This emphasize the additional contribution of free micelles to the dye transfer. On the other hand, the leakage in free micelles for both dialyzed or native NEs (green and blue curves, respectively), appears strictly identical whatever the temperature and the D/A ratio.

Summarizing this first screening, the stability of the encapsulation of lipophilic molecules solubilized in the core of nano-emulsion droplets appears potentially modulated by environmental factors. In the presence of an acceptor medium containing a lipid phase (as blank nano-emulsions), the dye leakage will exclusively be spread into the lipid compartment even in the presence of micelles. In the presence of micelles without acceptor lipid phase, micelles will receive a part of the dye, rapidly saturated. The leakage into micelles is dependent of their concentration (D/A ratio) and independent of the modification of temperature. As a last remark, the kinetics of all these phenomena are quite fast and globally comparable, comprised within 30 min. This shows that the main

factors that impacts on the equilibrium values are of thermodynamic origin rather than linked to kinetic phenomena. These first results are interesting since they disclose some important rules regarding the stability of nano-emulsions, which are in fact unstudied to date.

In order to confirm the relationship between color-shift and polarity of the acceptor observed above, NR668 was separately solubilized in all the systems studied: pure oil (VEA), solubilized in the core of NEs at different concentrations, in pure surfactant (Kolliphor® ELP), and in micellar suspension at different surfactant concentrations. The spectral properties (including values of the maximum of the peak, and the corresponding QYs, after an equilibration time of 300 min for all samples) are reported in Table 1. The spectra (normalized intensities and reported in the *Supplementary information* section as Fig. S5). These results confirm the color sensitivity of the NR668 towards the polarity of the solubilizing medium: solubilization in pure VEA appears as a low polarity limit with a peak around 550 nm, denoting a lipophilic environment. The emission spectra gradually shift to the red, first when formulated in nano-emulsions, and then in surfactants and in micelles, also affected by the concentration. These results confirm that the color shifts observed above in Fig. 2 (D,E,F) are effectively due to the leakage of the dye to either droplets or micelles (blue or red shift, respectively). In addition, when comparing the NEs formulations with increasing dye concentrations, the spectra are red-shifted. This is attributed to a better interaction with the bulk through a part already leaked in micelles present in the bulk, and/or a redistribution of the dye from (apolar) oil core towards the (more polar) droplet interface [6]. The information provided by the QY values in different conditions presented in Table 1 shows an interesting difference between the pure oil and the NE, even at similar concentrations, which seems to indicate that a significant part cannot be considered as solubilized in pure oil, or even has leaked to interface or water. Pure surfactant seems to be a medium relatively neutral that allows a solubilization of the dye. Finally, considering the micelles, shows the limitation in the solubility in such a medium, negligible when increasing the dye concentration above 1 wt.%.

Table 1 Maximum emission wavelength and quantum yield of NR668 solubilized in different media for various composition.

	3% in Pure oil (VEA)	1% in NEs	2% in NEs	3% in NEs	3% in Pure Surfactant	1% in Micelles	2% in Micelles	3% in Micelles
λ_{em} (nm)	563	594	602	606	608	616	626	628
QY (%)	86	68	47	41	59	39	7	1

Note: All samples were diluted before measurement to finally have a similar dye concentration of 1 µM.

Focus on the donor-to-acceptor ratio (D/A)

As discussed above, the chosen D/A has an effect on the NEs leakage. In Fig. 2, only a slight effect was observed, and in this section, we propose to explore it in depth. The system herein studied was the dialyzed, dye-loaded, NEs (in order to eliminate the interfering effect from free micelles). The acceptor medium was blank NEs, also dialyzed in the same conditions. Five different D/A values were

studied: 1/1, 1/2, 1/10, 1/20 and 1/50. All the experiments were conducted at 60° C.

The results are presented in Fig. 3, showing, as a function of time, the QY (Fig. 3 (A)), the shift of the fluorescent spectra (Fig. 3 (B)), and the nano-emulsion hydrodynamic diameter (Fig. 3 (C)). The fluorescence emission spectra of different D/A ratio, against time, corresponding to Fig. 3 (B) are reported in Fig. S6 in the *Supplementary information* section. In agreement with the observations above (Fig. 2), the QYs rose smoothly within a period of 100 min and then gradually stabilized within 300 min. It appears that the acceptor amounts significantly impacts on the kinetics and final stabilization values. The rise of QY values is accompanied by a significant blue-shift, indicating a migration towards the acceptor droplets. There are two reasons that explain this band shirt in Fig. 3 (B): first, at higher concentration, dye aggregation generally leads to formation of red shifted poorly emissive species; Second, at higher concentration, larger fraction of the dye is exposed to the interface of NEs. The latter increases environment polarity, which shifts to the red emission of NR668, because it is polarity sensitive probe [6]. Then, when the dye molecules are released into the acceptor oil droplets (*i.e.* diluted in oil), their local concentration in oil decreases and it results in a hypochromic shift (blue-shift) of the spectral peak Thus, the higher the number of acceptor droplets, the higher the amount of dye molecules leaked. On the other hand, the droplet size was conserved all along the leakage monitoring (Fig. 3(C)), the PDI values being below 0.2 for all measurements; that is a direct evidence of the droplet stability, but also of the fact that such a dye leakage is not due to Ostwald ripening, but to compositional ripening. After 10 days (for NR668-loaded nano-emulsions, 3 wt.% in oil), the QY value further increased by 6% and size increased by about 3 nm, coherent with the stabilization reported in the figures.

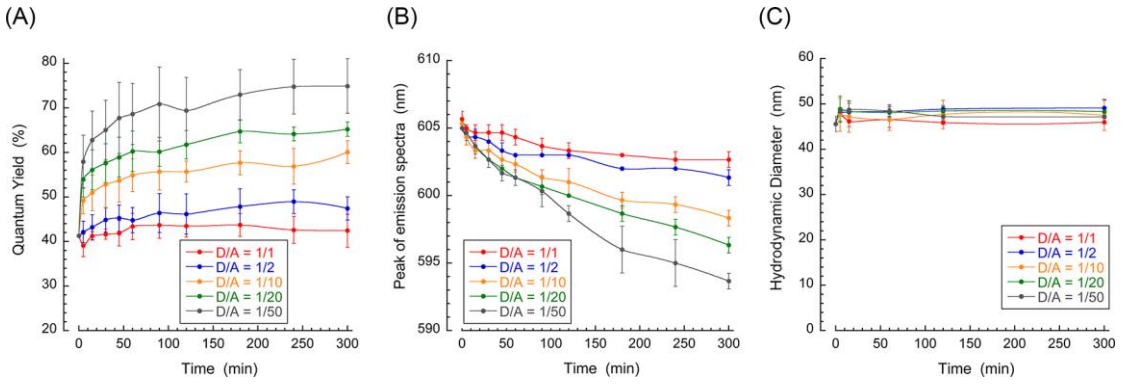

Figure 3: Evolution of quantum yield, maximum emission wavelength and size changes over the time with different donor-acceptor ratios (at constant temperature equal to 60° C, and dye concentration in oil equal to 3 wt.%). Data are mean values, and error bars indicate ± standard deviation, n = 3.

It follows therefrom that the encapsulated molecules leak towards the acceptor

site up to an equilibrium state is reached. However, this final state does not mean that we have reached a similar concentration between donor and acceptor droplets, but rather that a metastable state is reached respective to the temperature of the sample. For example, in Fig. 2 (B) and (C) for NEs, we can see that temperature impacts such an equilibrium. These saturating values with time indicate that an equilibrium is reached between donor and acceptor, and its variation with A/D ratio or temperature indicates that this equilibrium is modified. Thus, the concentrations of acceptor and donor, even at equilibrium, is not necessarily equalized. The dye leaking process seems to be limited by this final ratio between donor and acceptor, modulated by the temperature. To confirm this hypothesis, the effect of the temperature is specifically studied in the following section.

Focus on the effect of temperature

In the previous sections, temperature was shown to play an important role on the equilibrium between donor and acceptor. Herein we propose studying the leakage of NR668 from dialyzed loaded to dialyzed blank NEs (same conditions as in Fig. 3), but at different temperatures (25° C, 37° C, 60° C, 70° C and 80° C) and for three different D/A ratios (1/1, 1/10 and 1/50).

As regards the QYs (Fig. 4 (A,B,C)), the control in pure water remains very stable regardless of the temperature, up to 80° C. This is an important point since it proves the temperature stability of the NEs and of the dyes, excluding that any partial release can occur in water. The increase in the temperature results in higher QY variations, and thus in higher dye release. Kinetics are stabilized after about 1h-2h. As seen above in Fig. 3, increasing the donor-to-acceptor ratio also impacts on the QY values and thus on the dye release extent. However, the relationship between temperature and release appears gradual for the lower donor-to-acceptor ratio (D/A = 1/1), but reveals unexpected and atypical behavior for D/A = 1/10 and 1/50. In these latter cases, the dye release seems to obey to energetical thresholds, driven by the temperature and in which the systems remain blocked before the threshold are reached. For instance, in the case of D/A = 1/10, QY gradually increases up to 60% for T = 60° C, and jumps to 90% for 70° C and 80° C. This behavior is even more pronounced for 80° C, since for 25° C < T < 60° C all the QY values are roughly similar around 60% and for T > 70° C, they also jump up to 90%. As discussed in Fig. 2, all the kinetics are approximatively similar stabilized within 100 min whatever the D/A ratio and temperatures are, except the extreme point D/A = 50 or T > 70° C for which the curves are stabilized within 15 to 25 min.

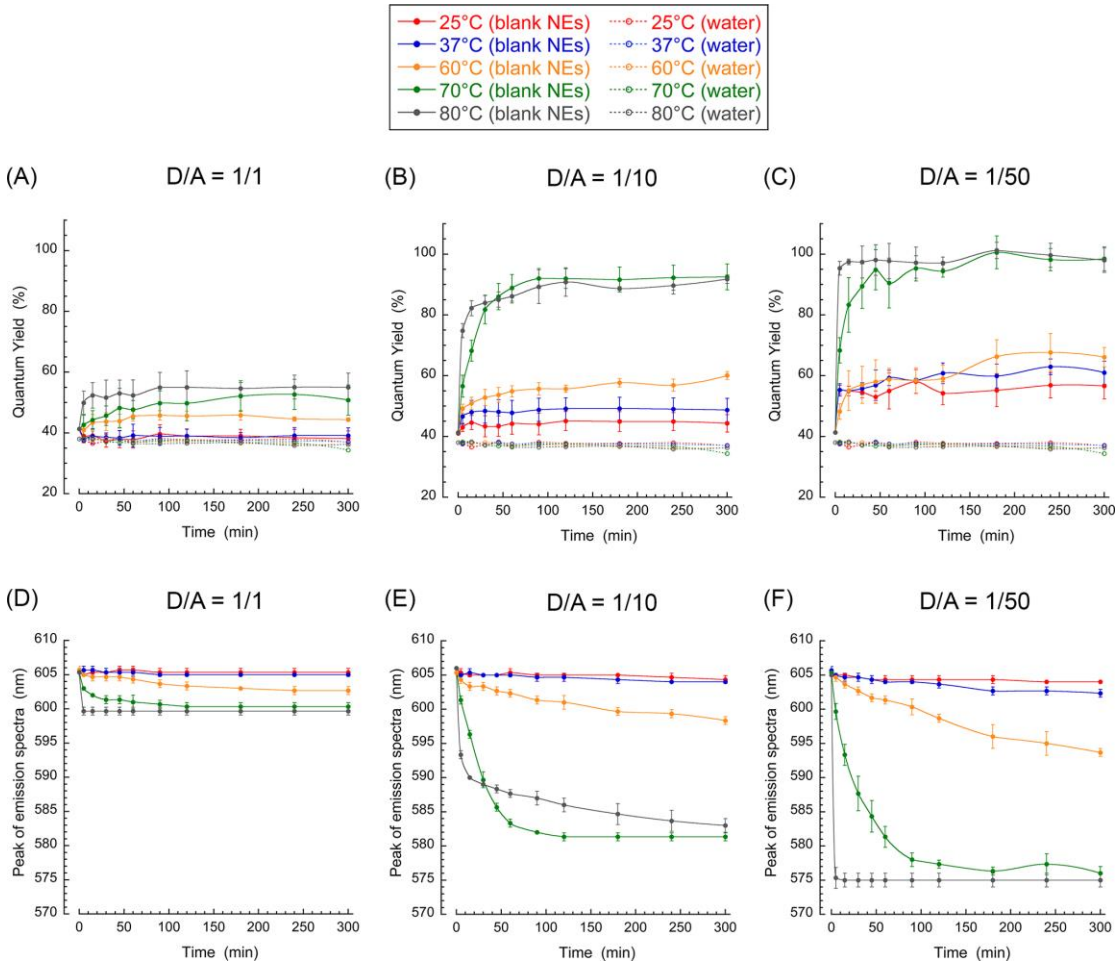

Figure 4: Evolution of the quantum yield (A,B,C) and the maximum emission wavelength (D,E,F) over the time and for different temperature (varying from 25° C to 80° C) and for three donor-to-acceptor ratio (1/1, 1/10 and 1/50), indicated on the figure, and dye concentration in oil equal to 3 wt.%. NR668 NEs (dialyzed) are brought in contact with blank NEs (dialyzed) or water (control). Data are mean values, and error bars indicate ± standard deviation, n = 3.

On the other hand, the peak shift of emission spectra, stabilized values and kinetics shown in Fig. 4 (D,E,F), are consistent with the variation of QY discussed above (corresponding spectra are reported in the *Supplementary information* section as Fig. S7, S8 and S9). The blue-shift confirms the dye leakage towards blank nano-emulsions. In addition, the follow-up of the droplet size and polydispersity in these experiments (reported in Fig. S10 in the *Supplementary information* section) are stable, proving that Ostwald ripening does not interfere with the dye release.

To summarize, these results confirmed the important effect of the D/A ratio on the dye leaking, and also the strong impact of the temperature on the ability of the dye to leak. However, the D/A ratio is a limiting factor, for which a small value (*e.g.* D/A = 1) prevents the dye escape even at high temperature. It seems that the limitation is defined by the acceptance capability of acceptor droplets, where increasing the number of droplets increases the potential leakage. On the

other hand, the fact that a temperature rise allows for increasing the release, with apparent thresholds (60° C), seems to indicate that temperature favors the inter-droplet molecular transfer. This behavior is likely related to the modification of the partial solubility of NR668 in water with the change of temperature. Water solubility increased with a temperature rise due to the kinetics energy that favors their intermolecular interactions with the aqueous molecules and shifts their equilibrium towards the bulk. This phenomenon was also observed in the presence of micelles in the bulk water in addition to the acceptor droplets, for non-dialyzed NEs (Fig. 2 red curve), that resulted in increasing the dye solubility in water.

This impact of temperature on the bulk solubility is thus expected to be progressive, and this is why it cannot be attributed to the gap observed between 60° C and 70° C. A possible explanation of this sudden dye release at high temperature is a complete fusion and re-emulsification of the droplets, because of the fact that the *cloud point* (CP) of this nonionic surfactant, Kolliphor ELP® (therefore related to the phase inversion temperature) is equal to 72.5° C (obtained for 1 wt.% aqueous solution) [32]. It follows that for T > CP, as classically described in the phase inversion temperature, the whole oil phase merges, and when temperature is brought back to room temperature, it is re-emulsified, with the dye spread over all droplets, and thus involving the QY values reaching 100%.

Focus on the dye concentration in oil droplets

The study of the dye loading also remains an important parameter on which it is worthwhile to focus. In fact, the mechanisms disclosed seem to be limited by a ratio of concentrations between the donor and the acceptor NEs, defined by the accepting capability of acceptor droplets or the partial solubility of dye in the bulk water surrounding the loaded droplets. Herein, 1 wt.%, 2 wt.% and 3 wt.% NR668-loaded NEs were prepared and used as donors, and two temperatures were compared, 60° C and 70° C.

Results are reported in Fig. 5, showing the QY and spectra peak shift variations (Fig. 5 (A) and Fig. 5 (B), respectively) as a function of time. Compared to all other results shown above, these ones present ΔQY and $\Delta\lambda_{em}$ (λ_{em} being the peak of emission spectra) as the difference between their measured values and the control in pure water. This representation is due to the fact that the baselines (values of the water control) is strongly impacted with the dye loading; thus, representing their relative variation allows a better comparison the dye leakages. Interestingly, in the case of these control experiments with pure water, increasing dye loading appears to have an important impact on both QY and spectral shift with any evolution over time (these raw data are reported in *Supplementary information* section, in Fig. S11). As a result, QYs are decreased (dashed lines in Fig. S11 (A,B)), which could be likely attributed to the fact that self-

quenching is accentuated with a concentration rise (*so-called* ACQ). The red-shift of the baselines is likely due to a higher dye localization to the droplets interface (excluding partition into micelles characterized by much higher environment polarity). Up to now, the dye concentrations were strictly identical for all experiments, and pure water as an acceptor media (as low as it is) was immediately saturated, and very stable, whatever the modifications of thermodynamic conditions.

In the presence of acceptor NEs, the spectroscopic changes depended on dye loading. As regards the values of ΔQYs (Fig. 5 (A)), the curves profiles gradually increase over time up to a plateau, indicating that the equilibrium of the dye redistribution was reached. Curves appear roughly similar for T = 60° C (stabilizing around ΔQY = 20%), but appear significantly different when T = 70° C, up to reaching ΔQY = 55% for 3 wt.% of dye in oil. Summary of these difference between T = 60° C and 70° C are shown in Fig. 5 (C), as the curves extrapolations for $t \rightarrow \infty$. When at 60° C the dye release is independent of the dye concentration, it significantly increases with the reservoir concentration at 70° C.

In the case of 60° C, the amount of material released seems similar whatever the concentration of the reservoir droplets: capability of acceptor medium is clearly the limiting factor as it was the case for D/A ratio (observed in Fig. 2, 3 and 4).

In contrast, at T = 70° C, the amount of released materials growths with the dye concentration in the reservoirs. In line with the conclusion drawn in the last section above the gap between 60° C and 70° C (for $T \geqslant CP$), this result is also consistent with a full repartition between all droplets, resulting in a re-emulsification of the droplets. The blue-shifts upon dye release followed similar trend as those for QY values (Fig. 5 (B)).

In this last series of experiments, we confirm that two complementary effects seem to drive the release of lipophilic molecules from lipid nano-emulsions reservoirs. They are *(i)* established equilibrium of dye release depends on the number of acceptor sites; and *(ii)* the modulation of this equilibrium, likely induced by presence of micelles in the medium, by the temperature and/or the dye concentration in the reservoirs. We think that such a conclusion is an interesting advance in the understanding of the nano-emulsion stability, herein accessed by simple, powerful and reliable methodology based on recording QY and position of the emission maximum.

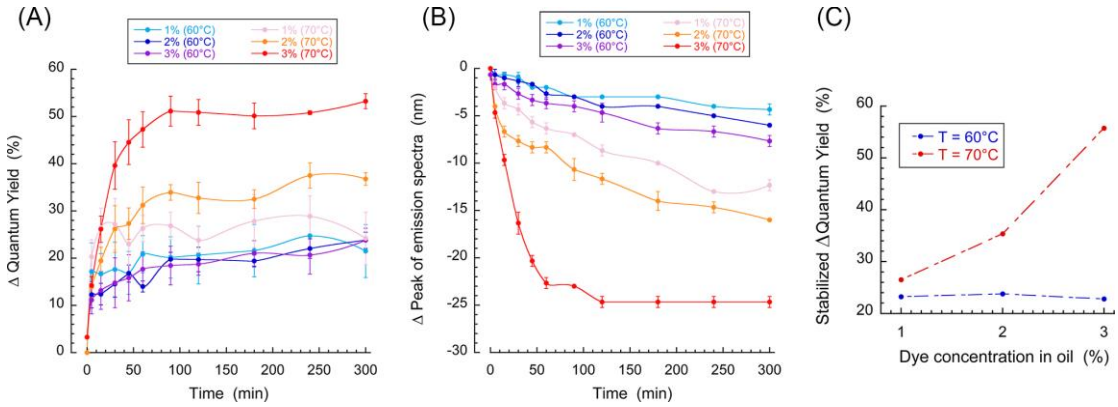

Figure 5: Study of the quantum yield (A) and values of the peak of the fluorescence spectra (B) for different dye concentrations in the oil core of nano-emulsions, and for two different temperatures, 60° C and 70° C with a D/A of 1/10. Data are mean values, and error bars indicate ± standard deviation, n = 3. (C) Extrapolations of the data from (A) and (B), for $t \rightarrow \infty$ (shown in Fig. S12 (E)).

Discussion

By definition, nano-emulsions are very stable in suspension compared to micro-scale emulsions. Only a slow phenomenon involving the mass transfer of the oil through the bulk medium is able to destabilize nano-emulsions. Differences in size and in composition between droplets are the origin of such an inter-droplet molecular transfer, because they induce a different chemical potential of the solute in each environment. As discussed above, reaching equilibrium passes through the ripening of the droplet suspension, so-called Ostwald or compositional ripening (a difference in droplet size or in composition initiates the process, respectively) [21, 33, 34]. As a result, nano-emulsions are considered kinetically stable but thermodynamically unstable (as the energy barrier of destabilization is reached). Ostwald ripening is widely described, studied, and modelized [11], and, by changing the composition of the oil core, it can be modulated and inhibited. On the other hand, when composition of the droplets is not uniform, it is not the difference in size but the concentration gradient that governs the inter-droplet mass exchange, eventually inducing modification in the droplet size and composition up to equilibrium [35, 36]. These both phenomena have been shown to be related to the mass transfer of the oil composing the droplets in the bulk, and to summarize, related to the droplet size distribution, composition distribution, solubility of the oil in the bulk, interfacial properties (*e.g.*, the barrier that inhibits the molecular transfer), but not related to the interfacial curvature (negligible effect on the difference in chemical potentials between two droplets) [11].

In addition to these considerations, Ostwald or compositional ripening implies that the own core of the droplets (oil phase), is released from one droplet, and able to migrate up to another droplet. On the other hand, nano-emulsions made with vegetable oils, natural products (like VEA as used in this study), or very

viscous oil, present a much better stability upon Ostwald ripening, even over months [10]. This was attributed to their very low water solubility, and/or to the fact that they are often a mixture of several components, breaking the mass transfer (since increasing the difference in chemical potentials of the less soluble species remaining in the droplets).

In this study, droplets are made with a viscous and water-insoluble oil (VEA) solubilizing a dye (NR668), which is highly lipophilic water-insoluble analogue of Nile Red. Thus, inter-droplet molecular transfer will only occur with the dye molecules (confirmed with the steadiness of the size over time when QY drastically changes, *e.g.*, in Fig. 3 (C) or Fig. S10). Accordingly, this dye release can legitimately be considered as compositional ripening, as it is originated by the same phenomenon (difference in composition), and as it follows the same rules, diffusing through the bulk water from droplet to droplet. Even if the dye is considered insoluble in water, an extremely low solubility still exists [11].

As the solubility of the solute (dye) is the critical factor in the release mechanisms, in order to understand the different results on dye release shown throughout the present study, let us consider its general expression, often considered to explain Ostwald ripening [11]:

$$C(r) = c(\infty) \cdot \exp\left(\frac{2\gamma V_m}{rRT}\right) \quad (2)$$

where $C(r)$ is the solubility of the droplet material (oil or dye) in a particle of radius r, $c(\infty)$ is the solubility in the bulk phase, γ is the surface tension, and V_m is the molar volume of the mobile compound. The expression $(2\gamma V_m/rRT)$ is assimilated to a characteristic length of the penetration of the solute in the bulk, around 1 nm for oil phase, but can be increased in relation of the affinities between encapsulated molecules and bulk phase.

The release experiments can be schematically represented in Fig. 6 (A), showing the donor and acceptor medium and the partial solubility of the dye in the bulk and its extent and limitations. Fig. 6 (B) shows the profile of solute concentrations in the reservoir droplets, through the interface (where interface does not induce resistance to mass transfer, as it is the case in nano-emulsions), and then, through the bulk where concentration decreases up to stabilize (as discussed in [35, 36]). However, in the presence of acceptor droplets, NR668 is again solubilized in their oil core, and fluorescence rose because of the change in solubilizing medium. As a result, the global amount of dye molecules in the total oil (donor plus acceptor) appears diluted, thus leading to an increase of the QY. In fact, even if the oil phase is still the dispersed phase in the form of droplets, the release from donors to acceptors through the water results in the fact that dye is diluted in the oil phase, considered as a whole. This explains the effect of the D/A ratio revealed above in Fig. 2, 3 and 4, when increasing the number of acceptors sites, the dilution increased. However, this

also means that the concentration in the acceptor droplets is limited and different from the reservoir. This means that donor and acceptor droplets are not in equilibrium with each other, but rather that acceptor droplets are in equilibrium with the bulk water.

In addition, analyzing Eq. (2) provides interesting considerations that we can correlate with our experimental results: *(i)* increasing the temperature has an impact on the value of $c(\infty)$ (Fig. 6 (C), effect of temperature) and thus on the concentration of the acceptor droplets (correlating with the representation of Fig. 6 (B)), as seen in Fig. 4; and *(ii)* increasing the concentration inside the droplets increases the characteristic length of penetration in the bulk (Fig. 6 (D), thus in line with the results of Fig. 5). It appears eventually that this theoretical representation of the dye transfer through its solubility in the bulk arises in direct correlation with the experimental results, therefore confirmed. These two factors, temperature and dye loading, significantly impact on the concentration of the dye in the bulk, thus impacting the release from donor droplets, and finally the loading of acceptor droplets.

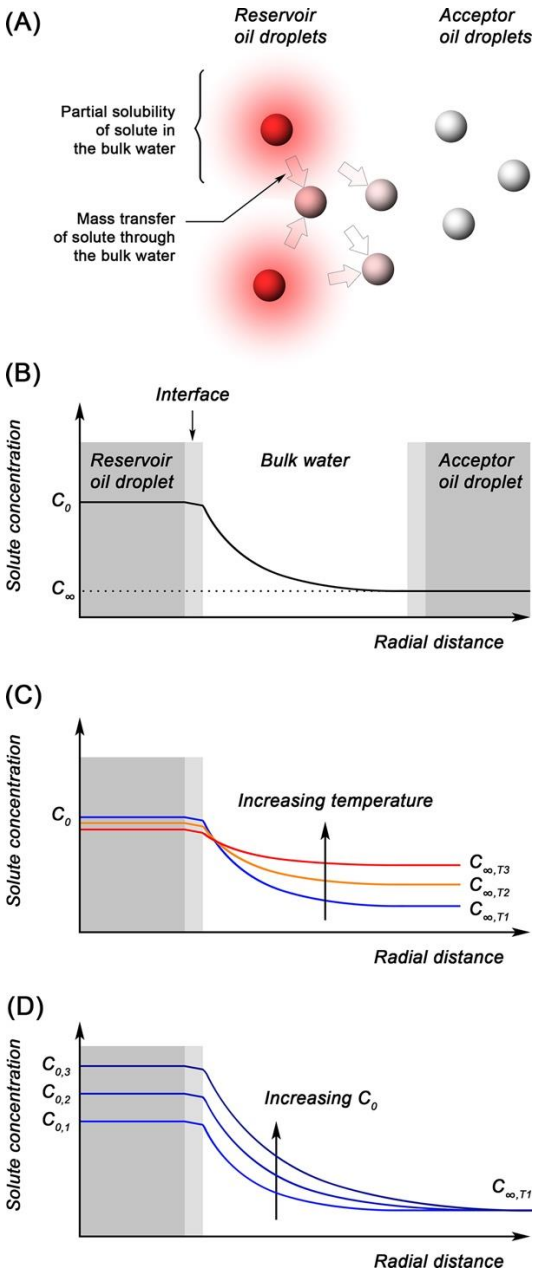

Figure 6: (A) Schematic representation of the molecular transfer mechanisms of dye between loaded (red) and blank (gray) nano-emulsion droplets. (B) Representation of the molecular concentration through the droplet interface and the bulk surrounding water, up to the acceptor droplet. (C) Effect of the temperature and (D) of dye concentration on this schematic profile.

Interestingly, when reporting the stabilized values of QYs plotted against the increase of acceptor droplets (acceptor to donor ratio), *e.g.*, in Fig. 7 (A) obtained from Fig. 3 (A) at $t \rightarrow \infty$, it appears that the evolution of the values follows a rising monoexponential trend that stabilized for the higher possible number of acceptors (for A/D $\rightarrow \infty$), about 75.2%. Under this point of view, Fig 7 (B) shows the impact of temperature on the full release capabilities of the loaded/empty droplet system. This representation more clearly represents the release behavior for the temperatures below 60° C, mainly considered as linked

to the modification of the solubility in the bulk (unlike for T ⩾ 70° C for which another mechanism seems involved). Interestingly, in contrast to the conclusions drawn for Ostwald ripening that can link the ripening rates to the temperature with an Arrhenius law [37] (thus, relating kinetics of mass transfer to the temperature), in this case, the transfer seems to reach an equilibrium after a stabilization within 300 min, with a value depending on the temperature. Thus, the molecular transfer of NR668 can reach a multitude of equilibriums related to the thermodynamic conditions and nature of acceptor. This is why these parameters do not have impact on the kinetics, making difficult to correlate our observations with a classical model.

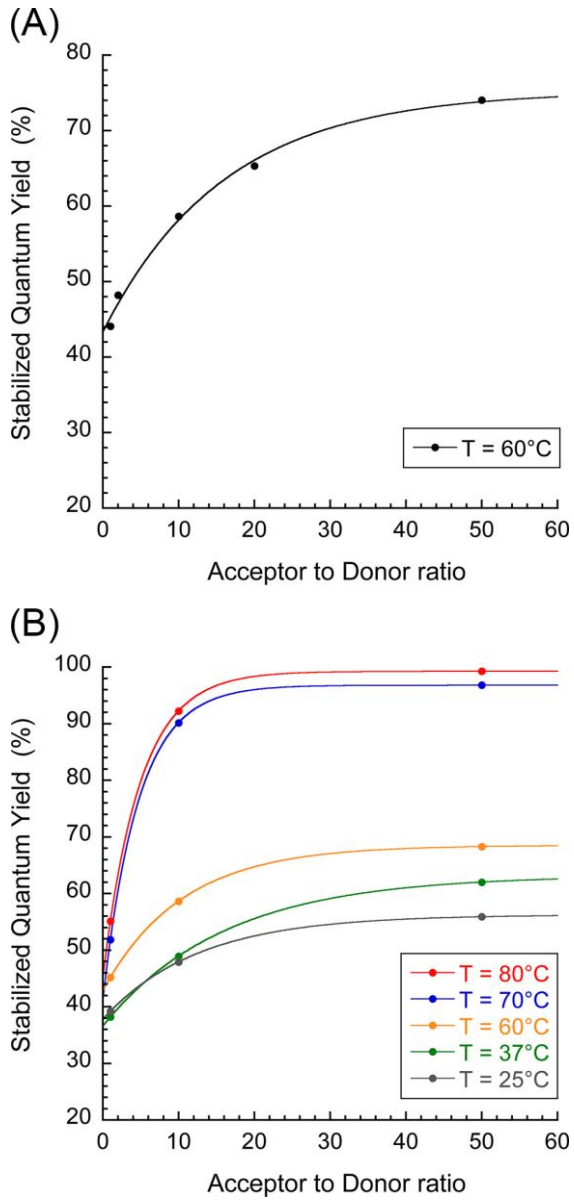

Figure 7: Synthesis of the trends obtained from extrapolation experimental data according to simple mono-exponential fits. (A) Data from Fig. 3 (extrapolations for t → ∞ shown in Fig. S12 (A)). (B) Data from Fig. 4 (extrapolations for t → ∞ shown in Fig. S12 (B),

(C) and (D)).

Conclusion

This study investigated the release mechanisms of a model fluorescent dye, from nano-emulsion droplets to acceptor media. Donor was nano-emulsions loaded with Nile red derivative NR668 and acceptor systems were pure water, micelles, or blank nano-emulsion droplets. Based on the aggregation-caused quenching (ACQ) that inhibits the dye brightness at high concentrations, our hypotheses were that, when released, the dyes will be diluted in the whole oil phase, improving their optical properties and thus the value of quantum yield of the sample. Thanks to this phenomenon, we proposed to elucidate the mechanisms driving the dye release from nano-emulsion droplets, and the potential impacts of the different formulation parameter on this release. Solvatochromism of NR668 revealed the modification of its solubilizing medium, as an additional indication of its release from donor nano-droplets. Innovation mainly lies in the combination of the simplicity of the experimental approach and its application to follow the inter-droplets interactions, which has never been reported to date. As key findings of this study, we showed that molecular transfer of encapsulated molecules follows the main rules of Ostwald or compositional ripening, and is mainly linked to the solubility of the solute in the bulk surrounding water. Acceptors solubilized a part of the dye, but at the bulk concentration, thus diluting the dye if we take the oil phase as a whole. This behavior disclosed that concentrations are not equalized between donors and acceptor droplets, but rather between bulk and acceptor droplets. Then, the modification of factors linked to the dye saturating concentration in the bulk (temperature or dye concentration) has a direct impact on the release from donor droplets towards water, and thus on the loading of acceptor droplets. To conclude, this study investigates the mechanisms governing the molecular transfer from nano-emulsion droplets, a theory based on the classical ripening but applied to a minor compound in the droplet composition. These results were often supposed [6,7,8,11,12,21] but, to the extent of our knowledge, never precisely studied to disclose the effective mechanisms in molecular transfer. Outlooks of such a work, beyond using blank nano-droplets as acceptor, would be applying this experimental approach to the study of dye release to living systems, biological membrane, cells or tissues.

Acknowledgments

The authors would like to acknowledge the financial support provided by King Abdulaziz City for Science and Technology (KACST), Grant no. 14-MED1472-10, as well the support from ERC Consolidator grant BrightSens 648528 and ANR BrightRiboProbes (ANR-16-CE11-0010), and finally the China Scholarship Council Ph.D. fellowship (CSC No. 201706240033) for the funding of Xinyue Wang.

References

[1] V.K. Rai, N. Mishra, K.S. Yadav, N.P. Yadav, Nanoemulsion as pharmaceutical carrier for dermal and transdermal drug delivery: Formulation development, stability issues, basic considerations and applications, J Control Release 270 (2018) 203-225.

[2] D. Pan, G.M. Lanza, S.A. Wickline, S.D. Caruthers, Nanomedicine: perspective and promises with ligand-directed molecular imaging, Eur J Radiol 70(2) (2009) 274-85.

[3] M.N. Yukuyama, D.D. Ghisleni, T.J. Pinto, N.A. Bou-Chacra, Nanoemulsion: process selection and application in cosmetics--a review, Int J Cosmet Sci 38(1) (2016) 13-24.

[4] M. Kah, T. Hofmann, Nanopesticide research: current trends and future priorities, Environ Int 63 (2014) 224-35.

[5] Ş. Yalçınöz, E. Erçelebi, Potential applications of nano-emulsions in the food systems: an update, Materials Research Express 5(6) (2018) 062001.

[6] A.S. Klymchenko, E. Roger, N. Anton, H. Anton, I. Shulov, J. Vermot, Y. Mely, T.F. Vandamme, Highly lipophilic fluorescent dyes in nano-emulsions: towards bright non-leaking nano-droplets, RSC Adv 2(31) (2012) 11876-11886.

[7] V.N. Kilin, H. Anton, N. Anton, E. Steed, J. Vermot, T.F. Vandamme, Y. Mely, A.S. Klymchenko, Counterion-enhanced cyanine dye loading into lipid nano-droplets for single-particle tracking in zebrafish, Biomaterials 35(18) (2014) 4950-7.

[8] X. Wang, N. Anton, P. Ashokkumar, H. Anton, T.K. Fam, T. Vandamme, A.S. Klymchenko, M. Collot, Optimizing the Fluorescence Properties of Nanoemulsions for Single Particle Tracking in Live Cells, ACS Appl Mater Interfaces 11(14) (2019) 13079-13090.

[9] M. Maruno, P.A.d. Rocha-Filho, O/W Nanoemulsion After 15 Years of Preparation: A Suitable Vehicle for Pharmaceutical and Cosmetic Applications, Journal of Dispersion Science and Technology 31(1) (2009) 17-22.

[10] F. Hallouard, N. Anton, G. Zuber, P. Choquet, X. Li, Y. Arntz, G. Aubertin, A. Constantinesco, T.F. Vandamme, Radiopaque iodinated nano-emulsions for preclinical X-ray imaging, RSC Advances 1(5) (2011) 792.

[11] T. Tadros, P. Izquierdo, J. Esquena, C. Solans, Formation and stability of nano-emulsions, Adv Colloid Interface Sci 108-109 (2004) 303-18.

[12] N. Anton, T.F. Vandamme, The universality of low-energy nano-emulsification, Int J Pharm 377(1-2) (2009) 142-7.

[13] N. Anton, T.F. Vandamme, Nano-emulsions and micro-emulsions: clarifications of the critical differences, Pharm Res 28(5) (2011) 978-85.

[14] R. Bouchaala, L. Richert, N. Anton, T.F. Vandamme, S. Djabi, Y. Mely, A.S. Klymchenko, Quantifying Release from Lipid Nanocarriers by Fluorescence Correlation Spectroscopy, ACS Omega 3(10) (2018) 14333-14340.

[15] C. Simonsson, G. Bastiat, M. Pitorre, A.S. Klymchenko, J. Béjaud, Y. Mély, J.-P. Benoit, Inter-nanocarrier and nanocarrier-to-cell transfer assays demonstrate the risk of an immediate unloading of dye from labeled lipid nanocapsules, European Journal of Pharmaceutics and Biopharmaceutics 98 (2016) 47-56.

[16] K.L. Markus Antonietti, Polyreactions in miniemulsions, Progress in Polymer Science 27(4) (2002) 689-757.

[17] B.P. Binks, J.H. Clint, P.D. Fletcher, S. Rippon, Kinetics of swelling of oil-

in-water emulsions, Langmuir 14 (1998) 5402-5411.
[18] W.I. Higuchi, M. Jagdish, Physical degradation of emulsions via the molecular diffusion route and the possible prevention thereof, Journal of pharmaceutical sciences (1961) 459-466.
[19] I.M. Lifshitz, V.V. Slyozov, The kinetics of precipitation from supersaturated solid solutions, Journal of Physics and Chemistry of Solids 19(1-2) (1961) 35-50.
[20] D.J. McClements, S.R. Dungan, J.B. German, J.E. Kinsella, oil exchange between oil-in-water emulsion droplets stabilised with a non-ionic surfactant, Food Hydrocolloids 6(5) (1992) 415-422.
[21] A.A. Peña, C.A. Miller, Kinetics of Compositional Ripening in Emulsions Stabilized with Nonionic Surfactants, Journal of Colloid and Interface Science 244(1) (2001) 154-163.
[22] A.-H. Ghanem, W.I. Higuchi, A.P. Simonelli, Interfacial Barriers in Interphase Transport: Retardation of the Transport of Diethylphthalate Across the Hexadecane-Water Interface by an Adsorbed Gelatin Film Journal of pharmaceutical sciences 58(2) (1969) 165-174.
[23] A.-H. Ghanem, W.I. Higuchi, A.P. Simonelli, Interfacial Barriers in Interphase Transport II: Influence of Additives upon the Transport of Diethylphthalate Across the Hexadecane-Gelatin-Water Interface, journal of pharmaceutical sciences 59(2) (1970) 232-237.
[24] A.-H. Ghanem, W.I. Higuchi, A.P. Simonelli, Interfacial barriers in interphase transport III: Transport of cholesterol and other organic solutes into hexadecane—gelatin—water matrices, Journal of pharmaceutical sciences 59(5) (1970) 659-665.
[25] B.P. Binks, P.D. Fletcher, B.L. Holt, O. Kuc, P. Beaussoubre, K. Wong, Compositional ripening of particle- and surfactant-stabilised emulsions: a comparison, Phys Chem Chem Phys 12(9) (2010) 2219-26.
[26] M.F. Haase, J. Brujic, Tailoring of high-order multiple emulsions by the liquid-liquid phase separation of ternary mixtures, Angew Chem Int Ed Engl 53(44) (2014) 11793-7.
[27] J. Otero, S. Meeker, P.S. Clegg, Compositional ripening of particle-stabilized drops in a three-liquid system, Soft Matter 14(19) (2018) 3783-3790.
[28] R. Bouchaala, L. Mercier, B. Andreiuk, Y. Mély, T. Vandamme, N. Anton, J.G. Goetz, A.S. Klymchenko, Integrity of lipid nanocarriers in bloodstream and tumor quantified by near-infrared ratiometric FRET imaging in living mice, Journal of controlled release 236 (2016) 57-67.
[29] D. Magde, G.E. Rojas, P.G. Seybold, Solvent dependence of the fluorescence lifetimes of xanthene dyes, Photochemistry and Photobiology 70(5) (1999) 737-744.
[30] A. Reisch, A.S. Klymchenko, Fluorescent Polymer Nanoparticles Based on Dyes: Seeking Brighter Tools for Bioimaging, Small 12(15) (2016) 1968-92.
[31] A.S. Klymchenko, Solvatochromic and fluorogenic dyes as environment-sensitive probes: design and biological applications, Accounts of chemical research 50(2) (2017) 366-375.
[32] R.C. Rowe, P.J. Sheskey, S.C. Owen, Handbook of pharmaceutical excipients, Pharmaceutical press London2006.

[33] P.C. Hiemenz, P.C. Hiemenz, Principles of colloid and surface chemistry, M. Dekker New York1986.
[34] A.S. Kabalnov, E.D. Shchukin, Ostwald ripening theory: applications to fluorocarbon emulsion stability, Advances in colloid and interface science 38 (1992) 69-97.
[35] D.J. McClements, S.R. Dungan, Factors that affect the rate of oil exchange between oil-in-water emulsion droplets stabilized by a nonionic surfactant: droplet size, surfactant concentration, and ionic strength, The Journal of Physical Chemistry 97(28) (1993) 7304-7308.
[36] J. Weiss, D.J. McClements, Mass transport phenomena in oil-in-water emulsions containing surfactant micelles: solubilization, Langmuir 16(14) (2000) 5879-5883.
[37] T. Delmas, H. Piraux, A.-C. Couffin, I. Texier, F. Vinet, P. Poulin, M.E. Cates, J. Bibette, How to prepare and stabilize very small nanoemulsions, Langmuir 27(5) (2011) 1683-1692.